

Coordinated Control of Multiple HVDC links using backstepping

Anne Mai Ersdal and Lars Imsland
Department of Engineering Cybernetics
Norwegian University of Science and Technology
anne.mai.ersdal@itk.ntnu.no
lars.imsland@itk.ntnu.no

Kjetil Uhlen
Department of Electric Power Engineering
Norwegian University of Science and Technology
kjetil.uhlen@elkraft.ntnu.no

Abstract—This article regards a power system containing multiple High Voltage Direct Current (HVDC) links. The topic is to exploit the HVDC lines' ability to control the power supplied by them to increase the stability of the system. The nonlinear controller-design method *backstepping* is applied to design a controller for the direct current (DC) through each HVDC link.

The simulation results show that the controller increases both transient stability and damping when some non-permanent errors are imposed on the system.

I. INTRODUCTION

The electric power systems in Europe today are complex dynamical systems of high dimension consisting of interconnected generators, transmission lines, loads etc. In order to keep the power supply safe and stable, it is important that all the generating units of an alternating current (AC) power system operate at the same frequency. The recent and ongoing liberalization of the energy market as well as increasing demand has in some cases reduced the stability margin of the power systems [1], and it has become important to augment their frequency stability.

Some of the possibilities for improving the power system stability are:

- i building new transmission lines,
- ii installing new generation capacity,
- iii better utilize the existing equipment in the power system.

High Voltage Direct Current (HVDC) links are in general used to transmit large amounts of energy over long distances. Norway is for example connected to the Netherlands and Denmark with underwater HVDC cables. But HVDC lines also have the ability of direct control of its power flow [2], and the current through already existing HVDC lines can therefore serve as a control input to help stabilize the AC network.

Improving system stability using a single HVDC link has been discussed in several papers, examples being [3] and [4]. Applying more than one HVDC link for stability improvement allows for coordinated control of the HVDC links, and perhaps improving the stability even more [5]. Coordinated control of several HVDC links is discussed in e.g. [5], [6] and [7].

Even though the current through the HVDC lines can be directly controlled, there are of course some restraints on both the amount of current that can pass, as well as the rate of change. The limitation on the power transmission capacity of HVDC lines is dominated by the maximum allowed conductor temperature [8]. The NorNed transmission line between Norway and the Netherlands, for example, has a capacity of 700 MW which is transferred at 450 kV. This gives a maximum current of approximately 780 A.

The problem investigated in this paper is inspired by the work of Eriksson et al. [5], on utilization of HVDC links to enhance system stability and dampen system oscillations. A major difference is that here the backstepping method will be applied in designing the nonlinear controller, instead of input-output exact linearization. Backstepping allows reduced control effort by not canceling damping terms.

The outline of the report is as follows. In Section II an overall system description is given, and the control problem is defined. Section III is devoted to designing the state feedback law using the backstepping method. The specific network used for simulation is presented in Section IV, along with the simulation results. These are then discussed in Section V and the conclusion is drawn in Section VI.

II. SYSTEM DESCRIPTION

Consider two separated power networks connected by p HVDC links. Each of the two power networks contains m and n nodes, respectively. Each of these nodes is connected to a synchronous generator and a load, which represents the equivalent of a larger, more complex network. Each of these separated networks can therefore represent networks of various size and complexity.

The swing equation for generator k is given as

$$\dot{\delta}_k = \omega_k \quad (1a)$$

$$\dot{\omega}_k = \frac{1}{M_k} (P_{mk} - \mathcal{R}e(E_{gk}I_{gk}^*) - D_k\omega_k) \quad (1b)$$

where δ_k is the rotor angle and ω_k the rotor angular velocity, both given in reference to the 50 Hz reference frame, P_{mk} the mechanical power produced by the turbine, $P_{ek} = \mathcal{R}e(E_{gk}I_{gk}^*)$ the electrical power acting on the rotor, E_{gk} the voltage of the internal bus, I_{gk} the

current from generator k , M_k the moment of inertia, and D_k the damping coefficient.

From (1), it can be shown that the set of nonlinear differential equations for several generators connected by a power grid and HVDC lines can be written

$$\dot{\delta} = \omega \quad (2a)$$

$$\dot{\omega} = \psi(\delta, \omega) + \phi(\delta) \mathbf{I}_{DC} \quad (2b)$$

where $\delta = [\delta_1 \ \cdots \ \delta_{m+n}]^T$, $\omega = [\omega_1 \ \cdots \ \omega_{m+n}]^T$, and \mathbf{I}_{DC} is a $p \times 1$ -vector containing the current through the HVDC lines. The connection between $\mathbf{I}_{DC} = [I_{DC,1} \ \cdots \ I_{DC,p}]^T$ and the currents from the generators $\mathbf{I}_G = [I_{g1} \ \cdots \ I_{g(m+n)}]^T$, is given by the algebraic equations for the network, and the procedure is explained in more detail in Section IV.

Since the networks are connected through DC lines, the frequencies can be different at each network. However, for stability reasons, they should be equal for the generators working together in the same AC grid. The purpose of the controller designed here is to make sure that this is fulfilled, by asymptotically stabilizing these generator frequency differences.

The system states to be stabilized for each AC network are therefore chosen as

$$\begin{aligned} \eta_{i1} &= \delta_{i1} - \delta_{i2} \\ &\vdots \\ \eta_{is-1} &= \delta_{i1} - \delta_{is} \\ \xi_{i1} &= \omega_{i1} - \omega_{i2} \\ &\vdots \\ \xi_{is-1} &= \omega_{i1} - \omega_{is} \end{aligned}$$

where $i = \{1, 2\}$ specifies the AC network, $s = \{m, n\}$ is the number of nodes in the AC network, and δ_{ij} and ω_{ij} are associated with the generator at node ij . The system dynamics for the two AC networks combined then become

$$\begin{aligned} \dot{\eta}_{ij} &= \xi_{ij} \\ \dot{\xi}_{ij} &= \Psi_{ij}(\eta_{ij}, \xi_{ij}, t) + \Phi_{ij}(\eta_{ij}, t) \mathbf{I}_{DC} \end{aligned}$$

With $\boldsymbol{\eta} = [\eta_{11} \ \cdots \ \eta_{1m} \ \eta_{21} \ \cdots \ \eta_{2n}]^T$ and $\boldsymbol{\xi} = [\xi_{11} \ \cdots \ \xi_{1m} \ \xi_{21} \ \cdots \ \xi_{2n}]^T$, we can collect

$$\dot{\boldsymbol{\eta}} = \boldsymbol{\xi} \quad (3a)$$

$$\dot{\boldsymbol{\xi}} = \boldsymbol{\Psi}(\boldsymbol{\eta}, \boldsymbol{\xi}, t) + \boldsymbol{\Phi}(\boldsymbol{\eta}, t) \mathbf{I}_{DC} \quad (3b)$$

where

$$\boldsymbol{\Psi}(\boldsymbol{\eta}, \boldsymbol{\xi}, t) = \begin{bmatrix} \Psi_{11}(\boldsymbol{\eta}, \boldsymbol{\xi}, t) \\ \vdots \\ \Psi_{1m}(\boldsymbol{\eta}, \boldsymbol{\xi}, t) \\ \Psi_{21}(\boldsymbol{\eta}, \boldsymbol{\xi}, t) \\ \vdots \\ \Psi_{2n}(\boldsymbol{\eta}, \boldsymbol{\xi}, t) \end{bmatrix}, \quad \boldsymbol{\Phi}(\boldsymbol{\eta}, t) = \begin{bmatrix} \Phi_{11}(\boldsymbol{\eta}, t) \\ \vdots \\ \Phi_{1m}(\boldsymbol{\eta}, t) \\ \Phi_{21}(\boldsymbol{\eta}, t) \\ \vdots \\ \Phi_{2n}(\boldsymbol{\eta}, t) \end{bmatrix}$$

It is not possible to write $\dot{\boldsymbol{\xi}}$ merely as a function of $\boldsymbol{\eta}$, $\boldsymbol{\xi}$ and \mathbf{I}_{DC} , there will also be dependencies on the original system variables ω and δ . This is solved by regarding δ and ω as time varying signals, hence the time-dependence in the system.

Since $\boldsymbol{\eta}$ does not necessarily have an equilibrium at the origin, a change of variables is made so that $\bar{\boldsymbol{\eta}} = \boldsymbol{\eta} - \boldsymbol{\eta}_0$:

$$\dot{\bar{\boldsymbol{\eta}}} = \boldsymbol{\xi} \quad (4a)$$

$$\dot{\boldsymbol{\xi}} = \boldsymbol{\Psi}(\bar{\boldsymbol{\eta}} + \boldsymbol{\eta}_0, \boldsymbol{\xi}, t) + \boldsymbol{\Phi}(\bar{\boldsymbol{\eta}} + \boldsymbol{\eta}_0, t) \mathbf{I}_{DC} \quad (4b)$$

where $\boldsymbol{\eta}_0$ is the equilibrium of (3a) and

$$\boldsymbol{\Psi}(\bar{\boldsymbol{\eta}} + \boldsymbol{\eta}_0, \boldsymbol{\xi}, t) = \boldsymbol{\Psi}_R(\bar{\boldsymbol{\eta}} + \boldsymbol{\eta}_0, \boldsymbol{\xi}, t) - \mathbf{D}\boldsymbol{\xi} \quad (5)$$

where $\mathbf{D}\boldsymbol{\xi}$ contains the ‘‘good’’ damping terms of $\boldsymbol{\Psi}(\bar{\boldsymbol{\eta}} + \boldsymbol{\eta}_0, \boldsymbol{\xi}, t)$, and $\boldsymbol{\Psi}_R(\bar{\boldsymbol{\eta}} + \boldsymbol{\eta}_0, \boldsymbol{\xi}, t)$ contains the remaining elements. The good damping terms consists of terms that provides desirable damping to the system states. The matrix \mathbf{D} is a $r \times r$ diagonal matrix containing combinations of $\frac{D_k}{M_k}$, where $r = m + n$.

The equilibrium of $\boldsymbol{\xi}$ is $\boldsymbol{\xi} = \mathbf{0}$, and the system (4) therefore has its equilibrium at the origin.

Assumption 1. *It is in the following assumed that $\boldsymbol{\Phi}(\bar{\boldsymbol{\eta}} + \boldsymbol{\eta}_0, t)$ is quadratic, that is, $\boldsymbol{\xi}$ and \mathbf{I}_{DC} have the same dimension, and invertible.*

This assumption is restrictive with regards to the configuration of the power system, and future work should include relaxing this assumption and considering a more general network configuration.

III. CONTROLLER DESIGN

Backstepping is a recursive procedure for designing nonlinear controllers. It requires full state feedback, and it is therefore assumed that all system states are either measured by phasor measurement units (PMU) or that they are estimated by a state estimator.

Consider systems on the form

$$\dot{\boldsymbol{\eta}} = \mathbf{f}(\boldsymbol{\eta}) + \mathbf{g}(\boldsymbol{\eta}) \boldsymbol{\xi} \quad (6a)$$

$$\dot{\boldsymbol{\xi}} = \mathbf{u} \quad (6b)$$

The idea behind backstepping is to break the design problem for the full system into a sequence of design problems for lower order subsystems [9]. First $\boldsymbol{\xi}$ is viewed as a virtual input to stabilize $\boldsymbol{\eta}$, then the stabilizing virtual input is ‘‘backstepped’’ through the integrator to find the actual input \mathbf{u} which stabilizes both $\boldsymbol{\eta}$ and $\boldsymbol{\xi}$.

Applying backstepping to systems on the form (6) is referred to as integrator backstepping [10]. Backstepping may also be applied to systems on the more general form

$$\dot{\boldsymbol{\eta}} = \mathbf{f}(\boldsymbol{\eta}) + \mathbf{g}(\boldsymbol{\eta}) \boldsymbol{\xi} \quad (7a)$$

$$\dot{\boldsymbol{\xi}} = \mathbf{f}_a(\boldsymbol{\eta}, \boldsymbol{\xi}) + \mathbf{g}_a(\boldsymbol{\eta}, \boldsymbol{\xi}) \mathbf{u} \quad (7b)$$

where $\boldsymbol{\eta}$ is known as the internal dynamics and $\boldsymbol{\xi}$ as the external dynamics. The external dynamics must have the

same dimension as the input \mathbf{u} , and it is convenient that the equilibrium point of the system is at the origin.

Since (4) is on this form, with \mathbf{I}_{DC} as input \mathbf{u} , we can design a controller for it using backstepping. This is summarized in the following Theorem, where we avoid canceling the “good” damping terms.

Theorem 1. *Under Assumption 1, the origin of (4) can be asymptotically stabilized by letting*

$$\mathbf{I}_{DC} = \Phi^{-1}(\bar{\boldsymbol{\eta}} + \boldsymbol{\eta}_0, t) \cdot [-\mathbf{K}_2^T \mathbf{z} - \bar{\boldsymbol{\eta}} - \Psi_R(\bar{\boldsymbol{\eta}} + \boldsymbol{\eta}_0, \boldsymbol{\xi}, t) - \mathbf{K}_1 \boldsymbol{\xi}] \quad (8)$$

where $\mathbf{z} = \boldsymbol{\xi} + \mathbf{K}_1 \bar{\boldsymbol{\eta}}$ and \mathbf{K}_1 and \mathbf{K}_2 are positive definite, constant matrices chosen such that

$$\mathbf{Q} = \begin{bmatrix} \mathbf{K}_1 & -0.5\mathbf{D}\mathbf{K}_1 \\ -0.5\mathbf{D}\mathbf{K}_1 & \mathbf{D}^T + \mathbf{K}_2 \end{bmatrix} \quad (9)$$

is positive definite.

Proof: Consider the Lyapunov function

$$V = 0.5\bar{\boldsymbol{\eta}}^T \bar{\boldsymbol{\eta}} + 0.5\mathbf{z}^T \mathbf{z} \quad (10)$$

where

$$\mathbf{z} = \boldsymbol{\xi} - \boldsymbol{\gamma}(\bar{\boldsymbol{\eta}}) \quad (11)$$

$$\boldsymbol{\gamma}(\bar{\boldsymbol{\eta}}) = -\mathbf{K}_1 \bar{\boldsymbol{\eta}} \quad (12)$$

Applying the controlled input \mathbf{I}_{DC} in (8) on the system (4) results in the following time derivative of the Lyapunov function

$$\dot{V} = -[\bar{\boldsymbol{\eta}}^T \quad \mathbf{z}^T] \begin{bmatrix} \mathbf{K}_1 & -0.5\mathbf{D}\mathbf{K}_1 \\ -0.5\mathbf{D}\mathbf{K}_1 & \mathbf{D}^T + \mathbf{K}_2 \end{bmatrix} \begin{bmatrix} \bar{\boldsymbol{\eta}} \\ \mathbf{z} \end{bmatrix} \quad (13)$$

$$= -\mathbf{q}^T \mathbf{Q} \mathbf{q} < 0 \quad (14)$$

Thus with (8) as input and (10) as Lyapunov function, it is clear that

i $V(\bar{\boldsymbol{\eta}}, \mathbf{z})$ is positive definite and decrescent with respect to $(\boldsymbol{\eta}, \boldsymbol{\xi})$,

ii $\dot{V}(\bar{\boldsymbol{\eta}}, \mathbf{z})$ is negative definite with respect to $(\boldsymbol{\eta}, \boldsymbol{\xi})$,

and according to Theorem 4.9 in [10], the origin of (4) is uniformly asymptotically stable. ■

IV. NETWORK EXAMPLE

Both the network model and the HVDC model described in the following are mainly based on those presented in [5], but differ somewhat in presentation. This section also serves to detail the modeling procedure outlined in Section II.

The network used for testing the controller is shown in Figure 1. It consists of four synchronous generators, four loads, four transmission lines and two HVDC links. This network model is a special case of the model presented in Section II, with $p = m = n = 2$. The detailed model of the HVDC lines and the AC network are presented in the following.

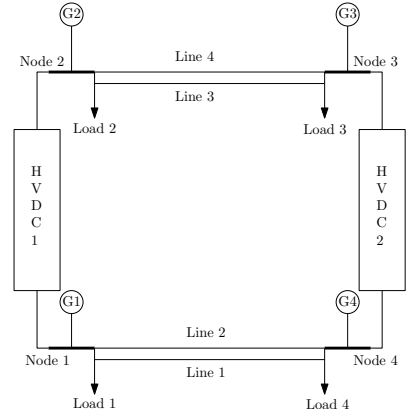


Fig. 1: Power system consisting of four synchronous machines and two HVDC links [5].

A. HVDC model

As in [5], the HVDC lines are of conventional type, meaning that reactive power is consumed by them and that the active power through them can be controlled via the DC current. It is assumed that the HVDC lines are lossless and have ideal control capabilities. It is also assumed that the power factors on both the inverter and rectifier side are equal. Positive direction for the current through HVDC link 1 and 2 are from node 1 to node 2 and from node 4 to node 3, respectively. This means that the current injected from the HVDC links have positive sign at node 2 and 3 and negative sign at node 1 and 4 of Figure 1.

Assuming that the absolute value of the node voltages at each side of the HVDC links are approximately equal, the injected current at node k by HVDC link l is given as

$$I_{HVDC,kl} = I_{DC,kl} \cdot e^{j\theta_k} \quad (15)$$

where θ_k is the voltage angle at node k , and $I_{DC,l}$ is the controlled DC current through HVDC link l . Assuming that node k is directly connected to HVDC link l , then $I_{DC,kl} = -I_{DC,l}$ if node k is at the rectifier side, and $I_{DC,kl} = I_{DC,l}$ if node k is at the inverter side. If node k and HVDC link l are not directly connected, $I_{DC,kl} = 0$.

Defining $I_{HVDC,k}$ as the total current injected at node k by both HVDC-links, leads to the following

$$\mathbf{I}_{HVDC} = \begin{bmatrix} I_{HVDC,1} \\ I_{HVDC,2} \\ I_{HVDC,3} \\ I_{HVDC,4} \end{bmatrix} = \begin{bmatrix} -e^{i\theta_1} & 0 \\ e^{i\theta_2} & 0 \\ 0 & e^{i\theta_3} \\ 0 & -e^{i\theta_4} \end{bmatrix} \mathbf{I}_{DC} \quad (16)$$

where $\mathbf{I}_{DC} = [I_{DC,1} \quad I_{DC,2}]^T$.

B. Network model

The algebraic equation for the current flow in the network is found using the internal node representation, where it is assumed that the loads in the network are constant resistances. Defining all currents as positive into

node k , Kirchoff's current law gives

$$I_{gk} + I_{Lk} + I_{HVDC,k} + \sum_{l=1}^{n+m} Y_{kl} U_l = 0 \quad (17)$$

where I_{gk} is the current injected by generator k , I_{Lk} the current from load k , $I_{HVDC,k}$ the current injected by the HVDC-links, Y_{kl} the systems admittance matrix at position (k, l) , U_l the voltage at node l , and $n + m$ the number of nodes in the network.

The current injected from generator k into node k is given by

$$I_{gk} = \frac{E_{gk} - U_k}{jx_{dk}}, \forall k = 1, \dots, 4 \quad (18)$$

where E_{gk} is the voltage at the internal bus of generator k , and x_{dk} is the generators transient reactance. The current from load k into node k is given by

$$I_{Lk} = -\frac{U_k}{R_k} \quad (19)$$

where R_k is the load resistance.

Combining (17)-(19) gives the following compact equation

$$\begin{bmatrix} \mathbf{I}_G \\ \mathbf{I}_{HVDC} \end{bmatrix} = \begin{bmatrix} \mathbf{Y}_A & \mathbf{Y}_B \\ \mathbf{Y}_C & \mathbf{Y}_D \end{bmatrix} \begin{bmatrix} \mathbf{E} \\ \mathbf{U} \end{bmatrix} \quad (20)$$

where $\mathbf{I}_G = [I_{g1} \ \dots \ I_{g4}]^T$. Eliminating \mathbf{U} from the equation yields

$$\begin{aligned} \mathbf{I}_G &= (\mathbf{Y}_A - \mathbf{Y}_B \mathbf{Y}_D^{-1} \mathbf{Y}_C) \mathbf{E} + \mathbf{Y}_B \mathbf{Y}_D^{-1} \mathbf{I}_{HVDC} \\ &= \mathbf{Y}_{RNM} \mathbf{E} + \mathbf{Y}_{HVDC} \mathbf{I}_{HVDC} \end{aligned} \quad (21)$$

Replacing I_{gk} in (1) with (21), and assuming that the absolute value of the generator's internal voltage $|E_{gk}|$ is constant, the system can be written as a set of nonlinear differential equations $\dot{\mathbf{x}} = \mathbf{h}(\mathbf{x}, \mathbf{I}_{DC})$:

$$\dot{\delta}_1 = \omega_1 \quad (22)$$

$$\dot{\delta}_2 = \omega_2 \quad (23)$$

$$\dot{\delta}_3 = \omega_3 \quad (24)$$

$$\dot{\delta}_4 = \omega_4 \quad (25)$$

$$\dot{\omega}_1 = \frac{1}{M_1} [P_{m1} - D_1 \omega_1 - G_{11} E_{g1}^2 \quad (26)$$

$$\begin{aligned} &- E_{g1} E_{g4} (B_{14} \sin(\delta_1 - \delta_4) + G_{14} \cos(\delta_1 - \delta_4)) \\ &+ E_{g1} (F_{11} \cos(\delta_1 - \theta_1) + K_{11} \sin(\delta_1 - \theta_1)) I_{DC,1} \\ &+ E_{g1} (F_{14} \cos(\delta_1 - \theta_4) + K_{14} \sin(\delta_1 - \theta_4)) I_{DC,2} \end{aligned}$$

$$\dot{\omega}_2 = \frac{1}{M_2} [P_{m2} - D_2 \omega_2 - G_{22} E_{g2}^2 \quad (27)$$

$$\begin{aligned} &- E_{g2} E_{g3} (B_{23} \sin(\delta_2 - \delta_3) + G_{23} \cos(\delta_2 - \delta_3)) \\ &- E_{g2} (F_{22} \cos(\delta_2 - \theta_2) + K_{22} \sin(\delta_2 - \theta_2)) I_{DC,1} \\ &- E_{g2} (F_{23} \cos(\delta_2 - \theta_3) + K_{23} \sin(\delta_2 - \theta_3)) I_{DC,2} \end{aligned}$$

$$\dot{\omega}_3 = \frac{1}{M_3} [P_{m3} - D_3 \omega_3 - G_{33} E_{g3}^2 \quad (28)$$

$$\begin{aligned} &- E_{g3} E_{g2} (B_{32} \sin(\delta_3 - \delta_2) + G_{32} \cos(\delta_3 - \delta_2)) \\ &- E_{g3} (F_{32} \cos(\delta_3 - \theta_2) + K_{32} \sin(\delta_3 - \theta_2)) I_{DC,1} \\ &- E_{g3} (F_{33} \cos(\delta_3 - \theta_3) + K_{33} \sin(\delta_3 - \theta_3)) I_{DC,2} \end{aligned}$$

$$\begin{aligned} \dot{\omega}_4 &= \frac{1}{M_4} [P_{m4} - D_4 \omega_4 - G_{44} E_{g4}^2 \quad (29) \\ &- E_{g4} E_{g1} (B_{41} \sin(\delta_4 - \delta_1) + G_{41} \cos(\delta_4 - \delta_1)) \\ &+ E_{g4} (F_{41} \cos(\delta_4 - \theta_1) + K_{41} \sin(\delta_4 - \theta_1)) I_{DC,1} \\ &+ E_{g4} (F_{44} \cos(\delta_4 - \theta_4) + K_{44} \sin(\delta_4 - \theta_4)) I_{DC,2}] \end{aligned}$$

where $Y_{RNM}(k, l) = G_{kl} + jB_{kl}$, and $Y_{HVDC}(k, l) = F_{kl} + jK_{kl}$, which easily can be written as (2). The system is then written as (4) with $\boldsymbol{\eta} = [\delta_2 - \delta_3 \ \delta_1 - \delta_4]^T$ and $\boldsymbol{\xi} = [\omega_2 - \omega_3 \ \omega_1 - \omega_4]^T$.

For this system, the "good" damping terms in \mathbf{D} of (5) is equal to

$$\mathbf{D} = \begin{bmatrix} \frac{D_2}{M_2} + \frac{D_3}{M_3} & 0 \\ 0 & \frac{D_1}{M_1} + \frac{D_4}{M_4} \end{bmatrix} \quad (30)$$

These contribute to stabilization, and the controller should therefore not cancel them.

Because of $I_{HVDC,kl}$'s dependency on θ_k , it is not possible to entirely eliminate the nodal voltages from the differential equations, but

$$\mathbf{I}_G = \mathbf{Y}_A \mathbf{E} + \mathbf{Y}_B \mathbf{U} \quad (31)$$

from (20) may be applied to find \mathbf{U} at each time step by knowledge of the previous \mathbf{I}_G and \mathbf{E} :

$$\mathbf{U}(t) = \mathbf{Y}_B^{-1} (\mathbf{I}_G(t-1) - \mathbf{Y}_A \mathbf{E}(t-1)) \quad (32)$$

C. Simulation

In this section the controller is tested with different types of faults imposed on the system. None of these faults are known beforehand. During the simulations, P_{mk} is kept constant for all generators, and the tuning parameters were in all four cases set to $\mathbf{K}_1 = 70\mathbf{I}$ and $\mathbf{K}_2 = 160\mathbf{I}$, where \mathbf{I} is the 2×2 identity matrix. The maximum current through the HVDC lines were set to be 1.5 pu.

Case A: First the controller is tested with no model-plant mismatch, and initial conditions outside the equilibrium. The simulation results with and without controller can be seen in Figure 2, and it shows that the controller clearly dampens the oscillations in a satisfying manner, and makes the system states converge.

Case B: Second, the controller is tested with the system fault identified as Case III in [5]: Load 4 is doubled for 100 ms at $t = 0.5$ s, while the controller is based on the nominal load. Figure 3 shows simulations with initial condition at the equilibrium, with and without controller. Clearly the controller handles the fault satisfyingly, by both decreasing the amplitude and eliminating oscillations.

Case C: Next, a fault similar to that identified as case II in [5] is introduced to the system. Here, line 4 has a three phase to ground error at $t = 0.5$ which lasts for 130 ms. The simulation results with and without controller, and with initial conditions at the equilibrium can be seen in Figure 4. The open-loop system diverges, but also here the controller performs well and stabilizes the system.

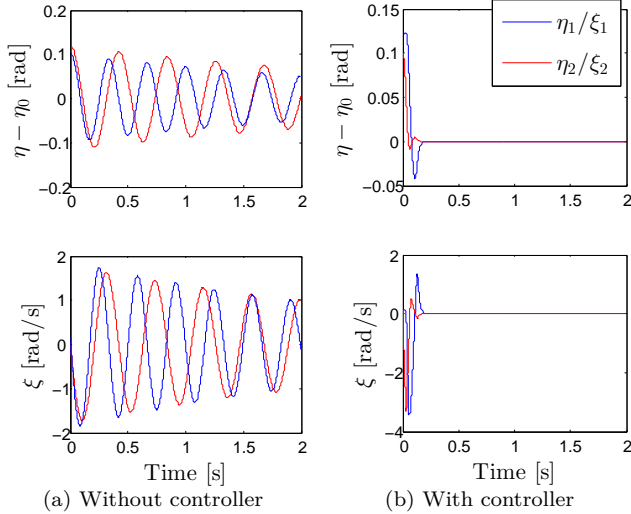


Fig. 2: Simulation results with error from Case A: Initial conditions outside the equilibrium.

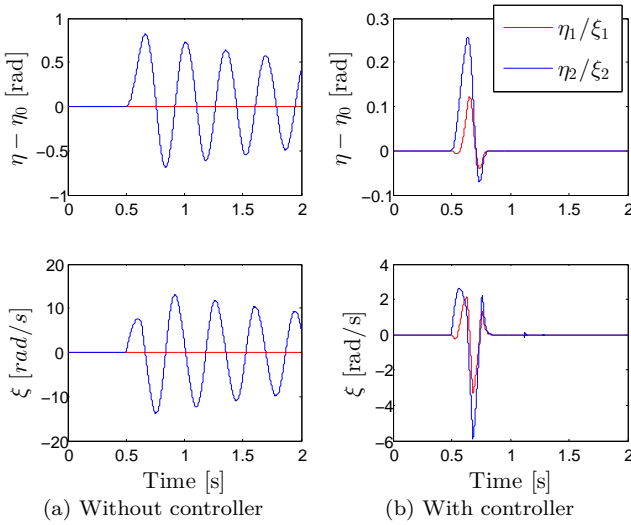


Fig. 3: Simulation results with error from Case B: Load 4 is doubled for 100 ms.

Case D: Last the controller was tested with a permanent fault of 5% increase in the load at node 4 occurring at $t = 0.5$ s. Since the fault is permanent the system's equilibrium is altered. This means that after $t = 0.5$ s, not only is the controller based on the wrong system model but it is also trying to control the system to a state that is no longer its equilibrium.

Figure 5 shows the results from the simulations with and without controller, and with initial conditions at the equilibrium. It shows that the controller manages to stabilize the system, however at an equilibrium different than that of the non-faulty system.

D. Current through the HVDC lines

For all the examples given above, the value of I_{DC} is saturated due to the limitation on power transmission

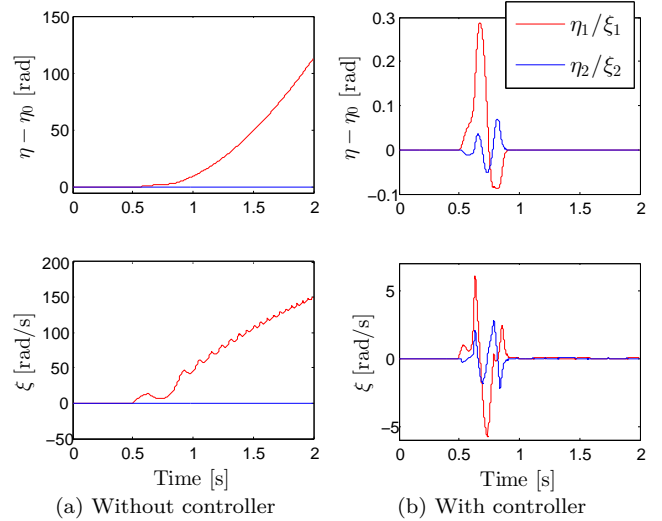


Fig. 4: Simulation results with error from Case C: Three phase to ground error in line 4.

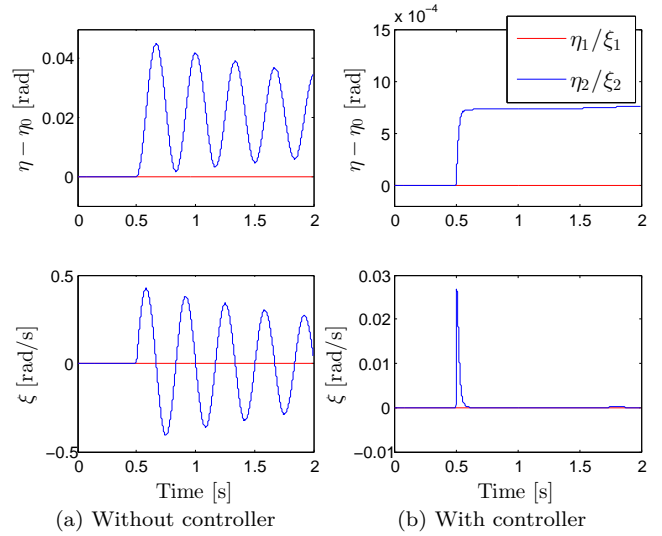


Fig. 5: Simulation results with error from Case D: Permanent 5% increase in load 4.

capacity. If one were to simulate without these limitations, one would see that the maximum value of I_{DC} is dominated by current peaks, often occurring during steady state. These peaks can also be seen when studying the input during simulations including saturation, but naturally their amplitude is then equal to the saturation limit. See for example Figure 6, which displays I_{DC} for Case B. It can be seen from Figure 3 that the system is at steady state from $t \approx 0.8$ s, and yet there are current peaks in the control signals at $t \approx 1.12$ s and $t \approx 1.28$ s.

V. DISCUSSION

When the faults imposed on the system only last for a short while, and the amount of time where the controller is based on the wrong system is relatively short, the controller both increases transient stability and

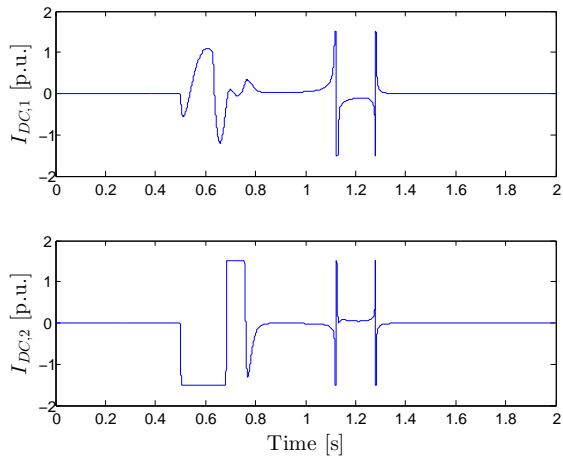


Fig. 6: I_{DC} from simulations with the error from Case B: Load 4 is doubled for 100 ms.

dampening of the system. This is because even though the Lyapunov function may grow during the fault, it is again guaranteed to sink from the time the fault has passed, hence bringing the system back to steady state.

When relatively small permanent faults are present, the controller brings the system to a new steady state. The reason for this is that the controller does not include integral control, resulting in a steady state error in η . However, for our control objective it does not matter where the equilibrium of η is.

There is no guarantee that the controller will increase stability in the case of arbitrarily large permanent faults. In order for the controller to handle larger permanent faults, the model should be properly updated when loads or network configuration change.

Due to the saturation in I_{DC} , it sometimes tends to rapidly shift between $\pm\sigma$ when stabilizing the system, where σ is the saturation limit. Since there in real life are limits on the current's rate of change as well, these instant shifts will rather be steep slopes limited by the current's maximum rate of change. How this will affect the controller is not investigated in this paper.

The peaks occurring during steady state in I_{DC} , seen in Figure 6, arise due to singularities in $\Phi(\bar{\eta} + \eta_0, t)$. These singularities appears at arbitrary moments in time, often during steady state, because of the changes in the generator angles $\delta_k(t)$. This means that Assumption 1 does not hold for these short moments. The peaks do not affect the system states when the system is at steady state. However, when the systems' equilibrium is altered due to permanent faults, and it is at steady state outside the origin, they lead to fluctuations from the equilibrium.

This is a significant problem with the presented controller. Even with saturation, eliminating the high amplitude of these peaks, they still cause trouble especially when there are permanent faults in the system. This is therefore an issue that needs to be further addressed, and is an important part of the further work that may be done with regards to this controller.

A nice feature of the presented controller which is not illustrated in the simulations, is that when I_{DC} does not reach saturation, only the part of the system that is subjected to fault is affected by the controller. The reason for this is simply that in the closed-loop dynamics, $\dot{\eta}_1$ and $\dot{\xi}_1$ are functions of η_1 and ξ_1 and $\dot{\eta}_2$ and $\dot{\xi}_2$ are functions of η_2 and ξ_2 . This means that the rest of the systems stays at steady state during a fault, while the “subsystem” where the fault occurred deals with the stabilization.

VI. CONCLUSION

The controller presented in this article is proven to asymptotically stabilize the system in theory, as long as the controller is based on the correct system. Simulations confirm that as long as the time the controller is based on an incorrect system is limited, it increases the stability of the system and brings it back to steady state.

It is also shown that during small permanent faults, the controller increases stability, but brings the system to a new equilibrium. However, it cannot necessarily handle arbitrary large permanent changes in the system. To address this issue the controller must work together with a good model updater, so that the model is updated when larger changes in loads or network configuration appears.

The main challenge of the presented controller is however the restrictive nature of Assumption 1, and the fact that the controller becomes singular for some combinations of generator angles. These singularities in the controller is an issue which must be resolved in order for the controller to function in practice. Another problem with Assumption 1 is of course that it confines the configuration of the network it may be applied on, demanding that the number of external variables ξ and the number of HVDC lines are equal.

REFERENCES

- [1] K. Morison, L. Wang, and P. Kundur, “Power System Security Assessment,” *Power & Energy magazine, IEEE*, vol. 2, no. 5, pp. 30–39, 2004.
- [2] J. Casazza and F. Delea, *Understanding Electric Power Systems*. IEEE Press, 2003.
- [3] T. Smed and G. Andersson, “Utilizing HVDC to Damp Power Oscillations,” *IEEE Transactions on Power Delivery*, vol. 8, no. 2, pp. 620–627, Apr. 1993.
- [4] X. Li, “A nonlinear emergency control strategy for HVDC transmission systems,” *Electric Power System Research*, vol. 67, no. 3, pp. 153–159, 2003.
- [5] R. Eriksson, V. Knazkins, and L. Söder, “Coordinated control of multiple HVDC links using input-output exact linearization,” *Electric Power Systems Research*, vol. 80, no. 12, pp. 1406–1412, Dec. 2010.
- [6] R. Eriksson and V. Knazkins, “On the Coordinated Control of Multiple HVDC Links: Modal Analysis Approach,” *GMSARN International Journal*, vol. 2, pp. 15–20, 2008.
- [7] L. Pilotto, M. Szechtman, A. Wey, W. Long, and S. Nilsson, “Synchronizing and damping torque modulation controllers for multi-infeed HVDC systems,” *IEEE Transactions on Power Delivery*, vol. 10, no. 3, pp. 1505–1513, Jul. 1995.
- [8] L. Weimers, “Bulk power transmission at extra high voltages, a comparison between transmission lines for HVDC at voltages above 600 kV DC and 800 kV AC .” 2000.
- [9] M. Krstić, I. Kanellakopoulos, and P. Kokotović, *Nonlinear and Adaptive Control Design*. John Wiley & Sons, Inc., 1995.
- [10] H. K. Khalil, *Nonlinear Systems*, 3rd ed. Prentice Hall, 2002.